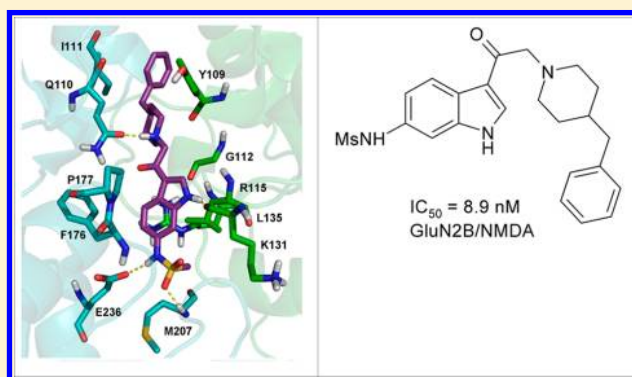


Synthesis and Biological Characterization of 3-Substituted
1*H*-Indoles as Ligands of GluN2B-Containing *N*-Methyl-D-aspartate
Receptors. Part 2Rosaria Gitto,^{*,†} Laura De Luca,[†] Stefania Ferro,[†] Maria R. Buemi,[†] Emilio Russo,[‡]
Giovambattista De Sarro,[‡] Mariangela Chisari,[§] Lucia Ciranna,^{||} and Alba Chimirri[†][†]Dipartimento di Scienze del Farmaco e Prodotti per la Salute, Università di Messina, Viale Annunziata, I-98168 Messina, Italy[‡]Dipartimento di Science of Health, Università Magna Graecia, Viale Europa Località Germaneto, I-88100 Catanzaro, Italy[§]Dipartimento di Biomedicina Clinica e Molecolare, Sezione di Farmacologia e Biochimica, Università di Catania, Viale Andrea Doria 6, I-95125 Catania, Italy^{||}Dipartimento di Scienze Bio-Mediche, Sezione di Fisiologia, Università di Catania, Viale Andrea Doria 6, I-95125 Catania, Italy

S Supporting Information

ABSTRACT: In the course of the identification of new indole derivatives targeting GluN2B-subunit-containing *N*-methyl-D-aspartate (NMDA) receptor, the (*N*-1*H*-indol-6-methanesulfonamide-3-yl)-2-(4-benzylpiperidin-1-yl)ethanone (**10b**) was identified as a potent ligand for this NMDA receptor subunit. It displays very high binding affinity (IC_{50} of 8.9 nmol) for displacement of [³H]ifenprodil, thus showing improved potency with respect to the previously reported analogues as confirmed by functional assay. This finding was consistent with the docking pose of compound **10b** within the binding pocket localized in the GluN1-GluN2B subunit interface of NMDA receptor tetraheteromeric complex.



INTRODUCTION

Most of the excitatory neurotransmission in the mammalian central nervous system is mediated by glutamate (Glu). Three different classes of postsynaptic ionotropic glutamate receptors (iGluRs) have been identified.^{1–5} Among them the *N*-methyl-D-aspartate (NMDA) receptors have gained much attention because of their implication in acute and chronic neurological diseases (among which are stroke, traumatic brain injury, neuropsychiatric disorders, dementia, and epilepsy).^{6–8} The tetraheteromeric structure of NMDA receptor contains two GluN1 subunits and two of the four possible GluN2 subunits (GluN2A–D) encoded by different genes.⁹ The four possible GluN2 subunits (GluN2A–D) are differently distributed among brain regions and contribute to functional diversity of NMDA receptors.^{10,11} It was demonstrated that antagonists targeting GluN2B-containing receptors could provide an opportunity to pharmacologically modulate NMDA receptor function for selected group of neurons, thus avoiding side effects that have so far limited the therapeutic utility of broad-spectrum NMDAR antagonists as neurotherapeutic agents.¹¹

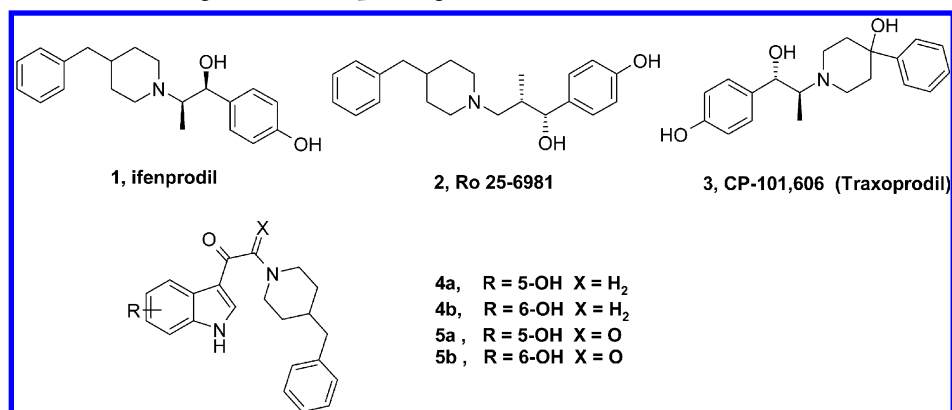
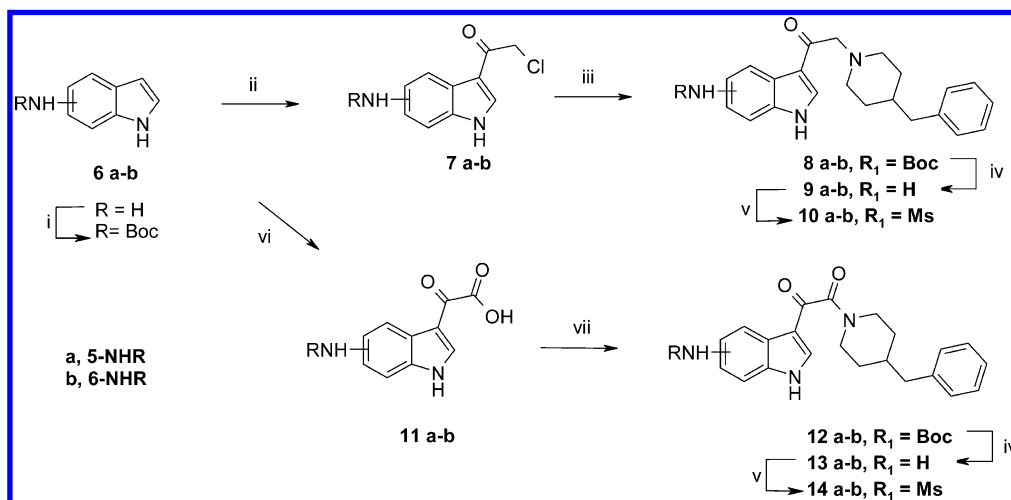
GluN2B subunit shows a modular architecture consisting of four discrete domains: an amino-terminal domain (ATD), a clamshell-like ligand binding domain (LBD), a transmembrane domain forming the ion pore, and an intracellular carboxy-terminal domain (CTD).¹ In the past years, significant progress

has been made in the identification of different classes of GluN2B subunit selective antagonists as allosteric modulators that interact with the extracellular amino-terminal domain (ATD).¹¹ The prototype of this class of ligands was the phenylethanolamine derivative **1** (ifenprodil),¹² which provided the starting point for developing new selective ligands. During the optimization process other ifenprodil-like compounds have been identified such as **2** (Ro 25-6981)¹³ and **3** (CP-101,606),¹⁴ which demonstrated more selectivity and wider safety profile.¹⁵ Notably, **3** showed efficacy in treatment of refractory major depressive disorder (phase 2 trials).^{16,17}

Subsequently extensive studies led to the identification of new chemical entities with a high degree of subunit selectivity. In this context, we reported a molecular modeling strategy useful for identifying several indole derivatives (**4**, **5**; Chart 1) as GluN2B ligands with IC_{50} values from 17 nM to 2.66 μ M.^{18–21} Interestingly, one of the most potent ligand (**4a**, Scheme 1) was able to prevent audiogenic seizures in DBA/2 mice and reduce NMDA receptor-mediated current recorded in patch clamp experiments from hippocampal neurons and also showed neuroprotective effects in HCN-1A cells.^{18,20}

Received: July 31, 2012

Chart 1. GluN2B Subunit-Containing NMDA Receptor Ligands

Scheme 1^a

^aReagents and conditions: (i) Boc₂O, diethyl ether, NaOH, rt 18 h; (ii) ClCH₂COCl, pyridine, dioxane, microwave 5 min, 50 °C, 200 W; (iii) 4-benzylpiperidine, K₂CO₃, DMF, microwave 10 min 50 °C, 200 W; (iv) DCM/TFA, rt 1 h; (v) MsCl, DCM, pyridine, rt 20 h; (vi) ClCOCOCl, diethyl ether, rt 2 h; (vii) 4-benzylpiperidine, HBTU, TEA, DMF, rt 2 h.

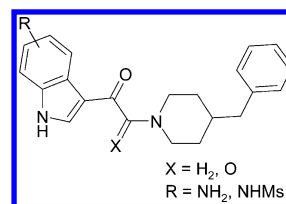
Then structure–activity relationship (SAR) analysis and molecular docking studies highlighted several structural requirements improving the recognition process into binding site. The obtained results were in good agreement with X-ray data that more recently demonstrated that the GluN1/GluN2B dimer interface represents the binding site for noncompetitive GluN2B subunit-selective NMDA receptor antagonists.^{22,23}

Herein we report the development of new indole derivatives that were designed to optimize the binding affinity and pharmacological activity of this class of ligands. The evaluation of binding affinity for displacement of [³H]ifenprodil, patch clamp experiments to test functional activity, and anticonvulsant screening were carried out to describe the biological profile of the new synthesized compounds. Moreover, to further rationalize the biological results, molecular docking studies have been performed.

RESULTS AND DISCUSSION

To enhance binding affinity and improve our understanding of SARs of this class of NMDA antagonists, we planned to synthesize eight new indoles (Chart 2). This structural optimization program started taking into account the binding poses in the ATD-binding site and SARs of other GluN2B-selective antagonists.¹⁵ Particularly, we focused on X-ray data of

Chart 2. Designed Ligands



GluN1-GluN2B ATD in complex with 1 and 2 (Protein Data Bank with accession codes 3QEL and 3QEM)²² and on our docking experiments.²¹ These studies revealed that the most GluN2B-selective antagonists interact with the binding site through specific aminoacidic residues in GluN1 and GluN2B subunits.²¹

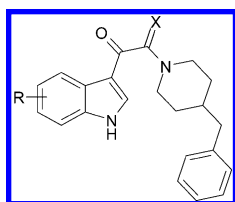
We attempted the isosteric and bioisosteric replacement of hydroxyl group of previously reported compounds 4a,b and 5a,b to investigate the role of H-bonding interaction and/or polar contacts with residue E236 (GluN2B) during the recognition process into the binding site. To this end, amino or methanesulfonamide substituent (R = NH₂ and NHMs, Chart 2) has been inserted at the C-5 or C-6 position. Moreover we substituted the ethanone linker with a 2-oxoethanone one, thus inducing the lowering of nitrogen

basicity to assess the role of the electrostatic interaction between the positive ionizable nitrogen atom (piperidine nucleus) and the carbonyl group of residue Q110 (GluN2B) within ifenprodil binding pocket.²²

Chemistry. The synthesis of target indole derivatives **9**, **10**, **13**, and **14** was accomplished as outlined in Scheme 1. The synthesis started from indoles as Boc-protected amine derivatives **6a,b**. By reaction of indoles **6a,b** with chloroacetyl chloride, we obtained intermediates **7a,b** which were coupled with benzylpiperidine to afford compounds **8a,b**. By treatment with DCM/TFA, compounds **8a,b** gave 1-(5-amino-1*H*-indol-3-yl)-2-(4-benzylpiperidin-1-yl)ethanone (**9a**) and 1-(6-amino-1*H*-indol-3-yl)-2-(4-benzylpiperidin-1-yl)ethanone (**9b**), which were converted into methanesulfonamide derivatives **10a,b**. The reaction of indoles **6a,b** with oxalylchloride yielded 2-(1*H*-indol-3-yl)-2-oxoacetic acids **11a,b**. In turn they were used as crude products for the coupling with benzylpiperidine using a standard amide coupling reaction to furnish Boc-protected aminoindoles **12a,b**. Finally, we prepared the desired 1-(amino-1*H*-indol-3-yl)-2-(4-benzylpiperidin-1-yl)-2-oxoethanones (**13a,b**) and (*N*-1*H*-indolmethanesulfonamide-3-yl)-2-(4-benzylpiperidin-1-yl)-2-oxoethanones (**14a,b**) by using the same procedure previously employed to obtain final compounds **9a,b** and **10a,b**. The chemical characterization of new indoles was supported by elemental analyses and spectroscopic measurements (see Experimental Section).

Biological Characterization. All synthesized compounds were evaluated for their ability to interact with the GluN2B subunit by testing [³H]ifenprodil binding inhibition,²⁴ and results were compared with those previously reported for **4a,b**, **5a,b**, and **1** (Table 1).

Table 1. GluN2B/NMDA Binding Affinities and Physicochemical Properties of Indole Derivatives (4, 5, 9, 10, 13, 14) and Reference Compound 1



compd	R	X	IC ₅₀ , μM ^a (inhibition at 10 μM)	LE ^b	LLE ^c	cLogD _{7.4} ^d
4a	5-OH	H ₂	0.025 ^e	0.41	3.79	3.81
4b	6-OH	H ₂	0.017 ^e	0.42	3.53	4.24
5a	5-OH	O	2.66 ^e	0.29	3.47	2.11
5b	6-OH	O	0.022 ^e	0.40	5.12	2.54
9a	5-NH ₂	H ₂	1.180	0.33	2.42	3.51
9b	6-NH ₂	H ₂	2.270	0.32	1.97	3.67
10a	5-NHMs	H ₂	0.320	0.31	2.78	3.71
10b	6-NHMs	H ₂	0.0089	0.39	4.35	3.70
13a	5-NH ₂	O	40%			1.84
13b	6-NH ₂	O	32%			2.00
14a	5-NHMs	O	42%			2.01
14b	6-NHMs	O	0.063	0.34	5.18	2.02
1	ifenprodil		0.020	0.45	5.37	2.33

^aDisplacement of [³H]ifenprodil.²⁴ ^bLE = -1.4 log IC₅₀/number of heavy atoms.^{25,26} ^cLLE = -log IC₅₀ - cLogD_{7.4}.²⁷ ^dcLogD_{7.4} data at pH 7.4 are predicted using a commercially available program (ACD/Labs).²⁸ ^eData from ref 19.

As shown in Table 1 the replacement of the hydroxyl substituent with an amino group gave derivatives **9a,b** and **13a,b** displaying significant decrease of binding affinity. We observed a similar behavior for the C-5 methanesulfonamide derivatives **10a** and **14a** (R = NHMs) when compared to compounds **4a** and **5a**, respectively, whereas 5-NHMs derivative **10a** was a more potent ligand than amino-substituted analogue **9a**. Notably, the presence of a methanesulfonamide substituent at the C-6 position gave better results. In fact the 6-NHMs-derivative **10b** showed the best IC₅₀ of 0.0089 μM that was about 2-fold more potent than that of the 6-hydroxyl analogue **4b** and about 250-fold more potent than that of the 6-NH₂-derivative **9b**. Among new 2-oxoethanones **13** and **14** (X = O) it was observed that the 6-NHMs derivative **14b** was the most active ligand, showing IC₅₀ of 0.063 μM, which was in good agreement with the result obtained for 6-substituted derivative **10b**. However, compound **14b** showed lower potency than 6-hydroxyl 2-oxoethanone analogue **5b** (see Table 1).

Overall the results of the binding affinity evaluation suggested that the optimization of binding affinity has been reached by introducing a methanesulfonamide substituent at C-6 position. In fact, among NHMs derivatives the 6-substituted compounds were the most active ligands (**10b** and **14b**). This behavior was in apparent discrepancy with previously reported SAR data, displaying very similar potency for the two ethanone derivatives C-5 and C-6 hydroxy-substituted (**4a** and **4b**, X = H₂), but it was in accordance with data obtained for 2-oxoethanone compounds (X = O), among which we found that C-5 substituted derivative **5a** was less active than C-6 analogue **5b**. So we can speculate that the substituent at C5/C6 position could play a relevant role during the molecular recognition to binding pocket. We postulate that this substituent could be able to make H-bonding interaction as donor moiety; however, its position seems very crucial for the optimization of binding affinity as explored through docking studies (vide infra).

In order to assess the role of lipophilicity for this class of GluN2B ligands, we calculated their ligand efficiency (LE) and lipophilic efficiency (LipE or LLE). In recent years LE and LLE^{26,27,29–31} have been shown to be useful tools in the lead optimization process. LE emerged as an approach to meaningfully interpret molecular size by balancing the size of the molecule against its potency. On the other hand LLE relates potency to lipophilicity, providing an estimate of the binding efficiency in the context of lipophilicity; therefore it has been used as an index of lipophilicity per unit of potency. LLE measures the extent to which binding is driven by specific hydrophobic effects (binding in a protein cavity as way to escape from solvent). Notably, an LE ranging from 0.3 to 0.5 characterizes a good drug candidate and compounds with LLE above 5 are usually considered highly optimized. As shown in Table 1, the most active indole derivatives exhibited promising LE and LLE values compared to compound **1**. In particular, compound **5b** exhibits significant LE (0.40) and excellent LLE (5.12) combined with cLogD_{7.4} of 2.54 considered optimal for drug developability. All these values are very similar to those of drug prototype **1**. Although the most potent ligand **10b** shows good LE (0.39), it displays high cLogD_{7.4} (3.70), thus generating lower LLE when compared to compounds **5b** and **14b** bearing the 2-oxoethanone linker. Interestingly, for compound **14b** we observed a good compromise between binding affinity (IC₅₀ = 63nM) and LLE (5.18). Among other

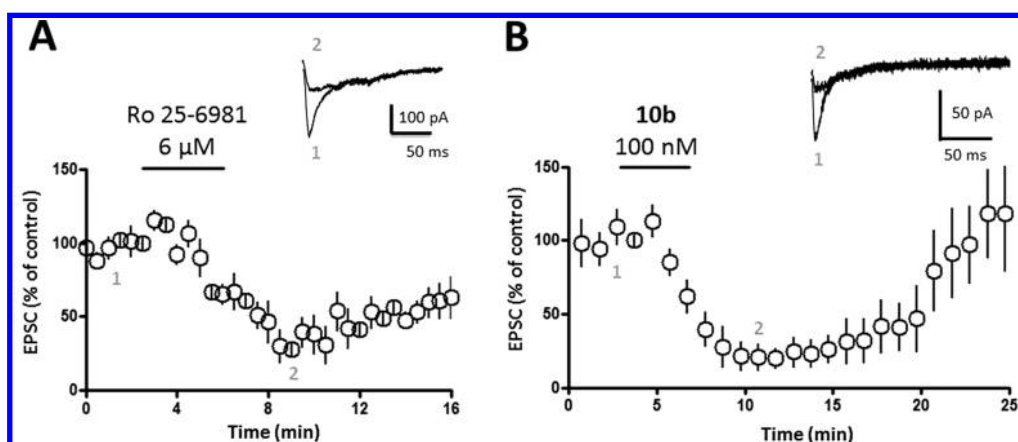


Figure 1. Compound **10b** behaves as an antagonist of GluN2B-containing NMDA receptors. Excitatory postsynaptic currents mediated by NMDA receptors (EPSC_{NMDA}) were recorded in mouse CA1 pyramidal neurons in Mg²⁺-free ACSF in the presence of CNQX (10 μM), glycine (10 μM), and bicuculline (5 μM). (A) EPSC_{NMDA} was inhibited by **2** (Ro 25-6981) (6 μM, 5 min), a selective antagonist of NMDA receptors containing the GluN2B subunit (EPSC_{NMDA} amplitude of 29 ± 11% of control (mean ± SEM, *n* = 5, *P* < 0.001). (B) Application of **10b** (100 nM, 5 min) reduced the amplitude of EPSC_{NMDA} to 23.3 ± 9% of control (mean ± SEM, *n* = 4, *P* < 0.0001). EPSC amplitude values are expressed as % of control amplitude. Pooled data of % EPSC values are plotted vs time. Insets (traces 1 and 2) show individual EPSCs from representative experiments.

derivatives, potent ligands **4a** and **4b** show excellent LE values (0.41 and 0.42, respectively); however, the high lipophilicity (cLogD_{7.4} > 3.5) reduces LLE values, thus compromising their drug developability.

On the basis of the observations described, we selected compound **10b** among other derivatives as a candidate for functional investigations on biological models (Figure 1). To evaluate the functional activity of the most potent ligand, **10b**, we used the patch clamp technique to record NMDA-mediated synaptic currents in mouse hippocampus, where GluN2B-containing NMDA receptors are expressed at high levels at early postnatal age.³² Excitatory postsynaptic currents (EPSCs) were recorded from CA1 neurons at a holding potential of −60 mV in Mg²⁺-free ACSF, in the presence of 6-cyano-7-nitroquinoxaline-2,3-dione (CNQX) (10 μM), glycine (10 μM), and bicuculline (5 μM). Application of D-AP5 (50 μM, 5 min) reduced EPSC amplitude to 28 ± 14% of control (*n* = 3, *P* < 0.0001), indicating that EPSCs were mediated by NMDA receptors (EPSC_{NMDA}). Application of **1** (10 μM, 5 min) induced a biphasic effect on EPSC_{NMDA} amplitude, with a transient increase (EPSC amplitude of 153 ± 24% of control, mean ± SEM, *n* = 3, *P* < 0.0001) followed by a reduction (EPSC of 79 ± 4% of control, mean ± SEM, *n* = 3, *P* < 0.001). Similar results were observed in previous studies showing that compound **1**, besides behaving as an antagonist of NMDA receptors, also increases NMDA receptor affinity for glutamate-site agonists and thus can either enhance or suppress NMDA-mediated effects.^{33,34} We next tested compound **2**, described as a high-affinity and selective blocker of GluN2B-containing NMDA receptors, with IC₅₀ values of 0.009 and 0.017 μM, respectively, for NR1C/NR2B and NR1F/NR2B subunit combination of NMDA receptors expressed in *Xenopus* oocytes.¹³ Application of **2** (6 μM, 5 min) reduced EPSC_{NMDA} amplitude to 29 ± 11% of control (mean ± SEM, *n* = 5, *P* < 0.001, Figure 1A), confirming that in our preparation the largest fraction of EPSC_{NMDA} amplitude was mediated by NMDA receptors containing the GluN2B subunit. Application of compound **10b** (100 nM, 5 min) reduced the amplitude of EPSC_{NMDA} to 23.3 ± 9% of control (mean ± SEM, *n* = 4, *P* < 0.0001; Figure 1B), which is comparable to the amount of inhibition induced by **2** at a maximally effective dose. The effect

of **10b** was fully reversible. A similar result was observed in rat CA1 neurons, in which application of **10b** (100 nM, 5 min) reversibly reduced EPSC_{NMDA} amplitude to 7.9 and 50% of control (*n* = 2).

To evaluate *in vivo* effects, all synthesized compounds were tested for their ability to prevent audiogenic seizures in DBA/2 mice.³⁵ In contrast to previous findings indicating that GluN2B subunit-containing receptor ligands such as **1**, **2**, and **4a** exhibit anticonvulsant effects,^{18,36} the new synthesized compounds are not able to demonstrate any efficacy (see Supporting Information). To understand the lack of *in vivo* efficacy, we calculated³⁷ the topological polar surface (TPSA), which is a relevant parameter to estimate compound polarity and to predict blood–brain barrier penetration.^{38,39} Drugs or candidates acting on CNS generally have optimal TPSA values estimated in the range 60–70 Å²; thus, the high TPSA value for the most active ligand **10b** (82.27 Å²) could explain the lack of *in vivo* efficacy due to its low capability to permeate the blood–brain barrier.

Computational Studies. To understand the effect of some of these modifications on GluN2B/NMDA receptor interactions, the docking poses within the GluN1/GluN2B interface for selected 6-substituted ligands (e.g., **4b**, **9b**, and **10b**) were examined (see Experimental Section). As shown in Figure 2A, the most active ligand **10b** (IC₅₀ of 8.9 nM) establishes a polar interaction with residue Q110 of GluN2B through the positive ionizable piperidine nitrogen atom. This ligand is also able to form hydrogen bonding interactions between the methanesulfonamide group at C-6 and residue E236 of GluN2B as well as between residue K131 of GluN1b and NH of the indole ring. Moreover, by means of the hydrogen bonding interaction between the oxygen atom and the backbone NH of M207, the mesyl functionality of **10b** occupies a further subpocket located at the bottom of dimeric interface (see Figure 2A). Finally, the benzylpiperidine portion and indole nucleus of ligand **10b** form hydrophobic interactions with some crucial residues on GluN1 (Y109, G112, L135) and GluN2B (I111, F176, P177). As seen in Figure 2B, we further examined the alignment of docking poses of the most potent ligand **10b** and other 6-substituted derivatives **4b** and **9b**. In spite of their different affinities in binding to GluN2B/NMDA receptor (see Table 1), we found

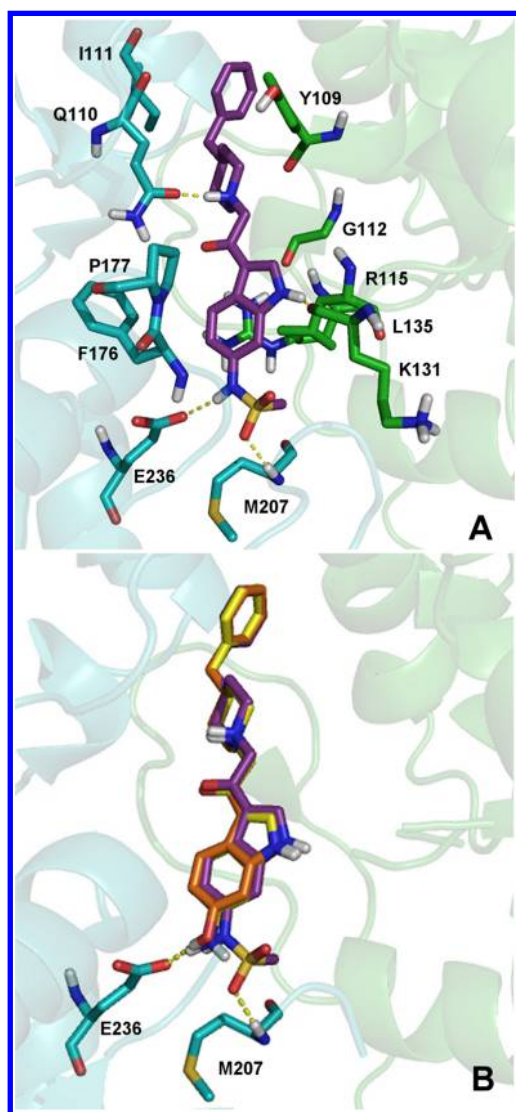


Figure 2. Docking poses of compounds **4b**, **9b**, and **10b** at the GluN1-GluN2B subunit interface (PDB code 3QEL): (A) binding of compound **10b** (magenta); (B) alignments of compounds **4b** (orange), **9b** (yellow), and **10b** (magenta). Important residues are drawn in stick and colored in cyan (GluN2B) and in green (GluN1). Hydrogen bonds (shown as dashed yellow lines) are formed between the compounds and GluN1-GluN2B subunit interface. The structures were prepared in PyMOL software.⁴⁰

that these three compounds share a very similar orientation and network of interactions within the GluN1/GluN2B interface. Particularly they seem to differ exclusively from the strength of hydrogen bonding interaction to the crucial residue E236 (GluN2B). Overall we can hypothesize that the lower potency of the 6-amino derivative **9b** (IC_{50} of 2.270 μM) compared to ligands **4b** (IC_{50} of 0.017 μM) and **10b** (IC_{50} of 0.0089 μM) could be related to the lack of a suitable chemical feature capable of being a good H-bond donor group to make a relevant interaction with E236. These findings were in good agreement with the pK_a values (calculated with ACD/Labs)²⁸ of the most active ligands. Thus, 6-hydroxyl derivative **4b** and 6-methanesulfonamide derivative **10b** possessed similar weak acid sites with pK_a values of 9.63 and 9.97, respectively. On the contrary the medium basicity of the 6-amino substituent of compound **9b** probably reduced the strength of the hydrogen

bonding donor interaction. Finally, the improvement of the potency of methanesulfonamide compound **10b** with respect to hydroxyl analogous **4b** could be explained considering the additional interaction with M207 which has been recently highlighted²³ as a very crucial residue during the recognition process into the GluN1/GluN2B interface of NMDA ATD.

CONCLUSIONS

As a continuation of our previous research, we designed and synthesized new 3-substituted-1*H*-indoles that proved to be highly potent ligands of GluN2B subunit-containing NMDA receptors. We considered as starting point the X-ray data of GluN1-GluN2B ATD in complex with **1** and **2** and our docking experiments. All synthesized compounds were evaluated for their ability to interact with the GluN2B subunit by testing [³H]ifenprodil binding inhibition. The best results were obtained with the 6-NHMs-derivative **10b** displaying an IC_{50} of 0.0089 μM , better than **1** and previously synthesized analogues (e.g., **4b**). Also functional assays confirmed this behavior, thus suggesting that the nature and position of the substituents could play a relevant role for the modulation of biological effects. Docking studies allowed us to postulate that the methanesulfonamide substituent at the C-6 position (**10b**) could be able to make H-bonding interaction as donor moiety. Moreover, the position of this substituent furnishes an additional interaction with M207 which has been recently highlighted as a very crucial residue during the recognition process into the GluN1/GluN2B interface of NMDA ATD. We show that compound **10b** displays high affinity and selective binding properties as well as a potent antagonist activity on GluN2B-containing NMDA receptors. Although **10b** does not exert any significant effect against audiogenic seizures in vivo (probably because of poor brain penetration, as estimated by TPSA calculation), this potent ligand might be a starting point for the design and development of new compounds showing more optimized physicochemical properties in CNS drug space.

EXPERIMENTAL SECTION

Chemistry. All starting materials and reagents commercially available (Sigma-Aldrich, Milan, Italy) were used without further purification. Microwave-assisted reactions were carried out in a CEM focused microwave synthesis system. Melting points were determined on a Stuart SMP10 apparatus and are uncorrected. Elemental analyses (C, H, N) were carried out on a Carlo Erba model 1106 elemental analyzer; the results confirmed a $\geq 95\%$ purity. Merck silica gel 60 F254 plates were used for analytical TLC; column chromatography was performed on Merck silica gel 60 (70–230 mesh). Flash chromatography (FC) was carried out on a Biotage SP₁ EXP. R_f values were determined on TLC plates using a mixture of CH₂Cl₂/CH₃OH (9:1) as eluent. ¹H NMR spectra were measured in CDCl₃ or dimethylsulfoxide-*d*₆ (DMSO-*d*₆) with a Varian Gemini 300 spectrometer. Chemical shifts are expressed in δ (ppm) and coupling constants (*J*) in Hz. All exchangeable protons were confirmed by addition of D₂O.

General Procedures for the Preparation of *tert*-Butyl 1*H*-Indolylcarbamates (6a,b**).** A solution of appropriate aminoindoles (396.0 mg, 3 mmol) with NaOH (7.5 mL, 1.6 M) was added to a solution of di-*tert*-butyl pyrocarbonate (Boc₂O) (720.0 mg, 3.3 mmol) in Et₂O (7.5 mL). The resulting mixture was stirred at room temperature overnight. The layers were separated and the organic phase was dried using dry Na₂SO₄, filtered, and concentrated under reduced pressure. The final compounds were purified by crystallization with Et₂O.

General Procedure for the Preparation of *tert*-Butyl [3-(Chloroacetyl)-1*H*-indolyl]carbamates (7a,b**).** The synthesis of

compounds **7a,b** has been carried out following a previously reported procedure²⁰ that has been optimized by means of the use of microwave irradiation. A mixture of chloroacetyl chloride (0.121 mL, 1.5 mmol) in dioxane (2 mL) was added dropwise to a solution of the appropriate Boc-protected amine derivatives (**6a,b**) (232 mg, 1 mmol) and pyridine (0.126 mL, 1.5 mmol) in dioxane (2 mL). The reaction mixture was placed in a cylindrical quartz tube (\varnothing , 2 cm), then stirred and irradiated in a microwave oven under the following conditions: 5 min, 50 °C, 200 W. Then the reaction was quenched with water (5 mL), and extraction was with EtOAc (3 × 10 mL). The combined organic layers were dried using Na₂SO₄, filtered, and concentrated to dryness in vacuo. The crude material was then subjected to silica gel chromatography by using cyclohexane/EtOAc (60:40).

General Procedure for the Preparation of Carbamates **8a,b**.

A DMF (2 mL) solution of the appropriate 3-chloroacetylindole derivative **7a,b** (308.4 mg, 1 mmol) and 4-benzylpiperidine (0.263 mL, 1.5 mmol) in alkaline medium by K₂CO₃ (70.0 mg, 0.5 mmol) was stirred and irradiated in a microwave oven under the following conditions: 10 min, 50 °C, 200 W. The reaction mixture was quenched with NaHCO₃ saturated aqueous solution (10 mL) and extracted with EtOAc (3 × 10 mL). The combined organic phases were washed with brine, dried over dry Na₂SO₄, filtered, and concentrated to dryness in vacuo. The crude material was purified by flash chromatography (FC) (DCM/CH₃OH, 9:1) and then crystallized by treatment with EtOH to give the desired products **8a,b**.

General Procedure for the Preparation of 1-(Amino-1H-indol-3-yl)-2-(4-benzylpiperidin-1-yl)ethanones (9a,b**).** A solution of TFA and DCM (1:1, 2 mL) was slowly added to cooled (0 °C) carbamates **8a,b** (447 mg, 1 mmol), and the mixture was stirred for 1 h at room temperature. Successively, the reaction mixture was quenched with H₂O (3 mL) and saturated aqueous NaHCO₃ solution (5 mL) and extracted with EtOAc (3 × 10 mL). The organic layer was dried (Na₂SO₄), combined, and concentrated in vacuo. The crude product was purified by flash chromatography (FC) (DCM/CH₃OH 9:1) and recrystallized by treatment with Et₂O to give the desired final products.

1-(5-Amino-1H-indol-3-yl)-2-(4-benzylpiperidin-1-yl)ethanone (9a**).** Yield 47%. Mp 148–150 °C, dec. $R_f = 0.15$. ¹H NMR (DMSO-*d*₆) (δ) 1.25–3.52 (m, 13H), 4.96 (bs, 2H, NH₂), 6.51–6.54 (dd, 1H, ArH, $J = 8.1$), 7.10–7.25 (m, 6H, ArH), 7.37 (s, 1H, ArH), 8.23 (s, 1H, H-2), 11.49 (bs, 1H, NH).

1-(6-Amino-1H-indol-3-yl)-2-(4-benzylpiperidin-1-yl)ethanone (9b**).** Yield 90%. Mp 142–144 °C, dec. $R_f = 0.11$. ¹H NMR (DMSO-*d*₆) (δ) 1.22–3.61 (m, 13H), 4.88 (bs, 2H, NH₂), 6.50–6.57 (d, 2H, ArH), 6.58 (s, 1H, ArH), 7.13–7.25 (m, 5H, ArH), 7.76–7.79 (dd, 2H, ArH), 8.14 (s, 1H, H-2), 11.29 (bs, 1H, NH).

General Procedure for the Preparation of (N-1H-Indolemethanesulfonamide-3-yl)-2-(4-benzylpiperidin-1-yl)ethanones (10a,b**).** Methanesulfonyl chloride (0.080 mL, 1.1 mmol) was added dropwise at 0 °C to a solution of appropriate amino derivatives **9a,b** (1 mmol) in DCM (3 mL) and in the presence of pyridine (0.089 mL, 1.1 mmol), under N₂ atmosphere. The reaction mixture was stirred overnight at room temperature, and the reaction was quenched with NaOH (6 N, 5 mL) and H₂O (3 mL). The layers were separated, and the aqueous phase was washed with DCM (3 × 5 mL). The aqueous layer was cooled (0 °C) and acidified to pH 2.0 by using 18% aqueous HCl. The obtained solid product was filtered and recrystallized by treatment with CH₃OH.

(N-1H-Indol-5-methanesulfonamide-3-yl)-2-(4-benzylpiperidin-1-yl)ethanone (10a**).** Yield 65%. Mp 212–214 °C, dec. $R_f = 0.23$. ¹H NMR (DMSO-*d*₆) (δ) 1.20–2.91 (m, 11H), 2.56 (s, 3H, CH₃), 3.44 (s, 2H, CH₂CO), 6.78–6.81 (dd, 1H, ArH, $J = 8.3$), 7.09–7.29 (m, 6H, ArH), 7.71 (s, 1H, ArH), 8.19 (s, 1H, H-2).

(N-1H-Indol-6-methanesulfonamide-3-yl)-2-(4-benzylpiperidin-1-yl)ethanone (10b**).** Yield 36%. Mp 160–162 °C, dec. $R_f = 0.17$. ¹H NMR (DMSO-*d*₆) (δ) 1.21–3.18 (m, 13H), 2.93 (s, 3H, Me), 7.10–7.30 (m, 6H, ArH), 7.42 (s, 1H, ArH), 8.07–8.09 (dd, 1H, ArH), 8.44 (s, 1H, H-2), 9.65 (bs, 1H, NH), 12.09 (bs, 1H, NH).

General Procedure for the Preparation of Carbamates **12a,b.** Oxalyl chloride (0.175 mL, 2 mmol) was added dropwise at 0 °C to a solution of appropriate Boc-protected aminoindoles **6a,b** (232 mg, 1 mmol) in Et₂O (5 mL). The reaction mixture was stirred at

room temperature for 2 h. A saturated aqueous NaHCO₃ solution (5 mL) was added to quench the reaction and the mixture was extracted with EtOAc (3 × 10 mL). The combined extracts were dried with Na₂SO₄ and concentrated in vacuo. A mixture of the crude compounds (1 mmol) and (HBTU) (379 mg, 1 mmol) in DMF (2 mL) was stirred for 30 min at room temperature. Successively, 4-benzylpiperidine (0.351 mL, 2 mmol) and TEA (0.139 mL, 1 mmol) were added. The reaction mixture was stirred for 2 h at room temperature. Then this mixture was quenched with H₂O (10 mL) and extracted with EtOAc (3 × 10 mL). The combined extracts were dried with dry Na₂SO₄ and concentrated in vacuo. The crude compound was purified by flash chromatography (FC) (DCM/CH₃OH, 96:4) and recrystallized from Et₂O.

General Procedure for the Preparation of 1-(Amino-1H-indol-3-yl)-2-(4-benzylpiperidin-1-yl)-2-oxoethanones (13a,b**) and (N-1H-Indolmethanesulfonamide-3-yl)-2-(4-benzylpiperidin-1-yl)-2-oxoethanone (**14a,b**).** By use of the same synthetic procedure previously described to obtain derivatives **9a,b** and **10a,b**, the desired compounds **13a,b** and **14a,b** have been synthesized.

1-(5-Amino-1H-indol-3-yl)-2-(4-benzylpiperidin-1-yl)-2-oxoethanone (13a**).** Yield 70%. Mp 147–150 °C, dec. $R_f = 0.56$. ¹H NMR (CDCl₃) (δ) 1.25–4.65 (m, 9H), 2.54–2.57 (d, 2H, $J = 6.69$), 6.65–7.65 (m, 7H, ArH), 7.72 (s, 1H, ArH), 7.73 (s, 1H, H-2), 10.10 (bs, 1H, NH).

1-(6-Amino-1H-indol-3-yl)-2-(4-benzylpiperidin-1-yl)-2-oxoethanone (13b**).** Yield 75%. Mp 128–130 °C, dec. $R_f = 0.50$. ¹H NMR (CDCl₃) (δ) 1.28–4.64 (m, 9H), 2.54–2.56 (d, 2H, $J = 6.87$), 6.52 (s, 1H, ArH), 6.68–6.71 (dd, 1H, ArH), 7.11–7.31 (m, 5H, ArH), 7.58–7.59 (s, 1H, H-2), 8.04–8.07 (dd, 1H, ArH), 9.34 (bs, 1H, NH).

(N-1H-Indol-5-methanesulfonamide-3-yl)-2-(4-benzylpiperidin-1-yl)-2-oxoethanone (14a**).** Yield 41%. Mp 121–123 °C, dec. $R_f = 0.66$. ¹H NMR (DMSO-*d*₆) (δ) 1.05–4.40 (m, 11H), 2.91 (s, 3H, Me), 7.15–7.51 (m, 7H, ArH), 8.01 (s, 1H, ArH), 8.11 (s, 1H, H-2), 9.54 (s, 1H, NH), 12.31 (bs, 1H, NH).

(N-1H-Indol-6-methanesulfonamide-3-yl)-2-(4-benzylpiperidin-1-yl)-2-oxoethanone (14b**).** Yield 35%. Mp 240–242 °C, dec. $R_f = 0.54$. ¹H NMR (DMSO-*d*₆) (δ) 1.05–4.39 (m, 11H), 2.91 (s, 3H, Me), 7.10–7.28 (m, 6H, ArH), 7.43 (s, 1H, ArH), 7.98–8.01 (dd, 1H, ArH, $J = 8.5$), 8.08 (s, 1H, H-2), 9.68 (bs, 1H, NH), 12.21 (bs, 1H, NH).

Receptor Binding Studies. The radioligand binding assays against NMDA receptor containing the GluN2B subunit were carried out using [³H]ifenprodil (Custom Screen by Ricerca Biosciences, U.S.).^{24,41} Cerebral cortices of male Wistar derived rats weighing 175 ± 25 g are used to prepare glutamate NMDA receptors in Tris-HCl buffer, pH 7.4. A 5 mg aliquot is incubated with 2 nM [³H]ifenprodil (plus 5 μ M GBR-12909 to block nonpolyamine sensitive sites) for 120 min at 4 °C. Nonspecific binding is estimated in the presence of **1** (10 μ M). Membranes are filtered and washed, and the filters are then counted to determine [³H]ifenprodil specifically bound. Three concentrations (in duplicate) of test compounds were used in the displacement assay.

Electrophysiology. Hippocampal slices were prepared from FVB mice and Wistar rats (postnatal PN age 10–15 days) as previously described,⁴² in accordance with the European Communities Council Directive of November 24, 1986 (86/609/EEC). The brains were removed, placed in oxygenated ice-cold artificial cerebrospinal fluid (ACSF; in mM: NaCl 124; KCl 3.0; NaH₂PO₄ 1.2; MgSO₄ 1.2; CaCl₂ 2.0; NaHCO₃ 26; D-glucose 10; pH 7.3), and cut into 300 μ m slices. Slices were continually perfused with oxygenated ACSF and viewed with infrared microscopy (Leica DMLFS). Schaffer collaterals were stimulated with negative current pulses (duration of 0.3 ms, delivered every 15 s by A310 Accupulser, WPI, U.S.). Evoked excitatory postsynaptic currents (EPSCs) were recorded under whole-cell configuration from CA1 pyramidal neurons (holding potential of –60 mV; EPC7-plus amplifier HEKA, Germany). Immediately after the beginning of recording, the slice was perfused with a Mg²⁺-free ACSF containing CNQX (10 μ M), glycine (10 μ M), and bicuculline (5 μ M) to isolate NMDA-mediated EPSCs. The recording electrode

was a glass micropipet (resistance, 1.5–3 M Ω) filled with intracellular solution (composition in mM: K-gluconate 140; HEPES 10; NaCl 10; MgCl₂ 2; EGTA 0.2; QX-314 1; Mg-ATP 3.5; Na-GTP 1; pH 7.3). Data were acquired and analyzed with Signal software (Cambridge Electronic Design, England). NMDA-mediated EPSC amplitude was measured as the difference between peak current and baseline. For each neuron studied, EPSC amplitude was measured during 5 min in control conditions and in the presence of compound **10b** and the two sets of values were compared using Student's unpaired *t* test (Graph Pad software).

Automated Molecular Docking Experiments. The crystal structure of amino terminal domains of the NMDA receptor subunit GluN1 and GluN2B in complex with **1** was retrieved from the RCSB Protein Data Bank (entry code 3QEL).²² The ligand and water molecules were discarded, and the hydrogen atoms were added to protein with Discovery Studio 2.5.⁴³ The structures of **1** and **2** were extracted from their X-ray complexes, and the other structures of the ligands (**4b**, **9b**, and **10b**) were constructed using Discovery Studio 2.5.⁴³ The conformational behavior of simulated compounds was investigated by a MonteCarlo procedure (as implemented in the VEGA suite of programs which generated 1000 conformers by randomly rotating the rotors).⁴⁴ All geometries obtained were stored and optimized to avoid high-energy rotamers. The 1000 conformers were clustered by similarity to discard redundancies; in this analysis, two geometries were considered nonredundant when they differed by more than 60° in at least one torsion angle. For each derivative, the lowest energy structure was then submitted to docking simulations. The ligands minimized in this way were docked in their corresponding proteins by means of Gold Suite 5.0.1. The region of interest used by Gold was defined in order to contain the residues within 15 Å from the original position of the ligand in the X-ray structure. The side chain of residue Leu135 was allowed to rotate according to the internal rotamer libraries in GOLD Suite 5.0.1. GoldScore⁴⁵ was chosen as a fitness function. The standard default settings were used in all the calculations, and the ligands were submitted to 100 genetic algorithm runs. The “allow early termination” command was deactivated. Results differing by less than 0.75 Å in ligand-all atom rmsd were clustered together. The best ranked GOLD-calculated conformation was used for analysis and representation.

■ ASSOCIATED CONTENT

● Supporting Information

Physicochemical and spectral data for intermediates **6a,b**, **7a,b**, **8a,b**, **12a,b**; anticonvulsant effects against sound-induced seizures in DBA/2 mice; [³H]ifenprodil binding curves of ligands **10b** and **14b**. This material is available free of charge via the Internet at <http://pubs.acs.org>.

■ AUTHOR INFORMATION

Corresponding Author

*Phone: +39 090 6766413. Fax: +39 090 6766402. E-mail: rgitto@unime.it.

Notes

The authors declare no competing financial interest.

■ ACKNOWLEDGMENTS

Financial support for this research by MiUR (Prin2008, Grant 20085HR5JK_002 and International Promotion of Young Researchers “Montalcini Program”) is gratefully acknowledged.

■ ABBREVIATIONS USED

ATD, amino-terminal domain; CTD, carboxy-terminal domain; DBA, dilute brown non-agouti; EPSC, evoked excitatory postsynaptic current; iGluR, ionotropic glutamate receptor; LBD, ligand binding domain; LE, ligand efficiency; LLE, lipophilic efficiency; TPSA, topological polar surface area

■ REFERENCES

- (1) Traynelis, S. F.; Wollmuth, L. P.; McBain, C. J.; Menniti, F. S.; Vance, K. M.; Ogden, K. K.; Hansen, K. B.; Yuan, H.; Myers, S. J.; Dingledine, R. Glutamate receptor ion channels: structure, regulation, and function. *Pharmacol. Rev.* **2010**, *62*, 405–496.
- (2) Mayer, M. L. Emerging models of glutamate receptor ion channel structure and function. *Structure* **2011**, *19*, 1370–1380.
- (3) Kumar, J.; Schuck, P.; Mayer, M. L. Structure and assembly mechanism for heteromeric kainate receptors. *Neuron* **2011**, *71*, 319–331.
- (4) Mayer, M. L. Glutamate receptor ion channels: Where do all the calories go? *Nat. Struct. Mol. Biol.* **2011**, *18*, 253–254.
- (5) Mayer, M. L. Structure and mechanism of glutamate receptor ion channel assembly, activation and modulation. *Curr. Opin. Neurobiol.* **2011**, *21*, 283–290.
- (6) Hedegaard, M.; Hansen, K. B.; Andersen, K. T.; Brauner-Osborne, H.; Traynelis, S. F. Molecular pharmacology of human NMDA receptors. *Neurochem. Int.* **2012**, *61*, 601–609.
- (7) Ogden, K. K.; Traynelis, S. F. New advances in NMDA receptor pharmacology. *Trends Pharmacol. Sci.* **2011**, *32*, 726–733.
- (8) Niciu, M. J.; Kelmendi, B.; Sanacora, G. Overview of glutamatergic neurotransmission in the nervous system. *Pharmacol., Biochem. Behav.* **2012**, *100*, 656–664.
- (9) Paoletti, P. Molecular basis of NMDA receptor functional diversity. *Eur. J. Neurosci.* **2011**, *33*, 1351–1365.
- (10) Mony, L.; Krzaczkowski, L.; Leonetti, M.; Le Goff, A.; Alarcon, K.; Neyton, J.; Bertrand, H. O.; Acher, F.; Paoletti, P. Structural basis of NR2B-selective antagonist recognition by N-methyl-D-aspartate receptors. *Mol. Pharmacol.* **2009**, *75*, 60–74.
- (11) Mony, L.; Kew, J. N.; Gunthorpe, M. J.; Paoletti, P. Allosteric modulators of NR2B-containing NMDA receptors: molecular mechanisms and therapeutic potential. *Br. J. Pharmacol.* **2009**, *157*, 1301–1317.
- (12) Carter, C.; Benavides, J.; Legendre, P.; Vincent, J. D.; Noel, F.; Thuret, F.; Lloyd, K. G.; Arbilla, S.; Zivkovic, B.; MacKenzie, E. T.; et al. Ifenprodil and SL 82.0715 as cerebral anti-ischemic agents. II. Evidence for N-methyl-D-aspartate receptor antagonist properties. *J. Pharmacol. Exp. Ther.* **1988**, *247*, 1222–1232.
- (13) Fischer, G.; Mutel, V.; Trube, G.; Malherbe, P.; Kew, J. N.; Mohacs, E.; Heitz, M. P.; Kemp, J. A. Ro 25-6981, a highly potent and selective blocker of N-methyl-D-aspartate receptors containing the NR2B subunit. Characterization in vitro. *J. Pharmacol. Exp. Ther.* **1997**, *283*, 1285–1292.
- (14) Chenard, B. L.; Bordner, J.; Butler, T. W.; Chambers, L. K.; Collins, M. A.; De Costa, D. L.; Ducat, M. F.; Dumont, M. L.; Fox, C. B.; Mena, E. E.; et al. (1S,2S)-1-(4-Hydroxyphenyl)-2-(4-hydroxy-4-phenylpiperidino)-1-propanol: a potent new neuroprotectant which blocks N-methyl-D-aspartate responses. *J. Med. Chem.* **1995**, *38*, 3138–3145.
- (15) Beinat, C.; Banister, S.; Moussa, I.; Reynolds, A. J.; McErlean, C. S.; Kassiou, M. Insights into structure–activity relationships and CNS therapeutic applications of NR2B selective antagonists. *Curr. Med. Chem.* **2010**, *17*, 4166–4190.
- (16) Preskorn, S. H.; Baker, B.; Kolluri, S.; Menniti, F. S.; Krams, M.; Landen, J. W. An innovative design to establish proof of concept of the antidepressant effects of the NR2B subunit selective N-methyl-D-aspartate antagonist, CP-101,606, in patients with treatment-refractory major depressive disorder. *J. Clin. Psychopharmacol.* **2008**, *28*, 631–637.
- (17) Skolnick, P.; Popik, P.; Trullas, R. Glutamate-based antidepressants: 20 years on. *Trends Pharmacol. Sci.* **2009**, *30*, 563–569.
- (18) Gitto, R.; De Luca, L.; Ferro, S.; Citraro, R.; De Sarro, G.; Costa, L.; Ciranna, L.; Chimirri, A. Development of 3-substituted-1H-indole derivatives as NR2B/NMDA receptor antagonists. *Bioorg. Med. Chem.* **2009**, *17*, 1640–1647.
- (19) Chimirri, A.; De Luca, L.; Ferro, S.; De Sarro, G.; Ciranna, L.; Gitto, R. Combined strategies for the discovery of ionotropic glutamate receptor antagonists. *ChemMedChem* **2009**, *4*, 917–922.

- (20) Gitto, R.; De Luca, L.; Ferro, S.; Occhiuto, F.; Samperi, S.; De Sarro, G.; Russo, E.; Ciranna, L.; Costa, L.; Chimirri, A. Computational studies to discover a new NR2B/NMDA receptor antagonist and evaluation of pharmacological profile. *ChemMedChem* **2008**, *3*, 1539–1548.
- (21) Gitto, R.; De Luca, L.; Ferro, S.; Buemi, M. R.; Russo, E.; De Sarro, G.; Costa, L.; Ciranna, L.; Prezzavento, O.; Arena, E.; Ronsisvalle, S.; Bruno, G.; Chimirri, A. Synthesis and biological characterization of 3-substituted-1*H*-indoles as ligands of GluN2B-containing *N*-methyl-D-aspartate receptors. *J. Med. Chem.* **2011**, *54*, 8702–8706.
- (22) Karakas, E.; Simorowski, N.; Furukawa, H. Subunit arrangement and phenylethanolamine binding in GluN1/GluN2B NMDA receptors. *Nature* **2011**, *475*, 249–253.
- (23) Burger, P. B.; Yuan, H.; Karakas, E.; Geballe, M.; Furukawa, H.; Liotta, D. C.; Snyder, J. P.; Traynelis, S. F. Mapping the binding of GluN2B-selective NMDA receptor negative allosteric modulators. *Mol. Pharmacol.* **2012**, *82*, 344–359.
- (24) Ricerca Biosciences. <http://www.ricerca.com>.
- (25) Bembenek, S. D.; Tounge, B. A.; Reynolds, C. H. Ligand efficiency and fragment-based drug discovery. *Drug Discovery Today* **2009**, *14*, 278–283.
- (26) Reynolds, C. H.; Tounge, B. A.; Bembenek, S. D. Ligand binding efficiency: trends, physical basis, and implications. *J. Med. Chem.* **2008**, *51*, 2432–2438.
- (27) Leeson, P. D.; Springthorpe, B. The influence of drug-like concepts on decision-making in medicinal chemistry. *Nat. Rev. Drug Discovery* **2007**, *6*, 881–890.
- (28) ACD/Labs, version 8.0; Advanced Chemistry Development, Inc.: Toronto, Ontario, Canada, 2004; www.acdlabs.com/.
- (29) Perola, E. An analysis of the binding efficiencies of drugs and their leads in successful drug discovery programs. *J. Med. Chem.* **2010**, *53*, 2986–2997.
- (30) Nicholls, A.; McGaughey, G. B.; Sheridan, R. P.; Good, A. C.; Warren, G.; Mathieu, M.; Muchmore, S. W.; Brown, S. P.; Grant, J. A.; Haigh, J. A.; Nevins, N.; Jain, A. N.; Kelley, B. Molecular shape and medicinal chemistry: a perspective. *J. Med. Chem.* **2010**, *53*, 3862–3886.
- (31) Moussa, I. A.; Banister, S. D.; Beinat, C.; Giboureau, N.; Reynolds, A. J.; Kassiou, M. Design, synthesis, and structure–affinity relationships of regioisomeric *N*-benzyl alkyl ether piperazine derivatives as sigma-1 receptor ligands. *J. Med. Chem.* **2010**, *53*, 6228–6239.
- (32) Loftis, J. M.; Janowsky, A. The *N*-methyl-D-aspartate receptor subunit NR2B: localization, functional properties, regulation, and clinical implications. *Pharmacol. Ther.* **2003**, *97*, 55–85.
- (33) Zhang, X. X.; Bunney, B. S.; Shi, W. X. Enhancement of NMDA-induced current by the putative NR2B selective antagonist ifenprodil. *Synapse* **2000**, *37*, 56–63.
- (34) Zhang, X. X.; Shi, W. X. Dynamic modulation of NMDA-induced responses by ifenprodil in rat prefrontal cortex. *Synapse* **2001**, *39*, 313–318.
- (35) de Sarro, G.; Chimirri, A.; De Sarro, A.; Gitto, R.; Grasso, S.; Giusti, P.; Chapman, A. G. GYKI 52466 and related 2,3-benzodiazepines as anticonvulsant agents in DBA/2 mice. *Eur. J. Pharmacol.* **1995**, *294*, 411–422.
- (36) Gitto, R.; De Luca, L.; De Grazia, S.; Chimirri, A. Glutamatergic neurotransmission as molecular target of new anticonvulsants. *Curr. Top. Med. Chem.* **2012**, *12*, 971–993.
- (37) Molinspiration Cheminformatics. Cheminformatics on the Web. <http://www.molinspiration.com/> (Molinspiration property engine, 2012).
- (38) Alavijeh, M. S.; Chishty, M.; Qaiser, M. Z.; Palmer, A. M. Drug metabolism and pharmacokinetics, the blood–brain barrier, and central nervous system drug discovery. *NeuroRx* **2005**, *2*, 554–571.
- (39) Pajouhesh, H.; Lenz, G. R. Medicinal chemical properties of successful central nervous system drugs. *NeuroRx* **2005**, *2*, 541–553.
- (40) *The PyMOL Molecular Graphics System*; Schrodinger, LLC: New York.
- (41) Schoemaker, H.; Allen, J.; Langer, S. Z. Binding of [³H]-ifenprodil, a novel NMDA antagonist, to a polyamine-sensitive site in the rat cerebral cortex. *Eur. J. Pharmacol.* **1990**, *176*, 249–250.
- (42) Costa, L.; Trovato, C.; Musumeci, S. A.; Catania, M. V.; Ciranna, L. 5-HT(1A) and 5-HT(7) receptors differently modulate AMPA receptor-mediated hippocampal synaptic transmission. *Hippocampus* **2012**, *22*, 790–801.
- (43) *Discovery Studio*, version 2.5; Accelrys Software, Inc.: San Diego, CA, 2009.
- (44) Pedretti, A.; Villa, L.; Vistoli, G. VEGA: a versatile program to convert, handle and visualize molecular structure on Windows-based PCs. *J. Mol. Graphics Modell.* **2002**, *21*, 47–49.
- (45) Jones, G.; Willett, P.; Glen, R. C.; Leach, A. R.; Taylor, R. Development and validation of a genetic algorithm for flexible docking. *J. Mol. Biol.* **1997**, *267*, 727–748.